Volume 10, Issue 2, 2020, 4977 - 4981 ISSN 2069-5837
Biointerface Research in Applied Chemistry
www.BiointerfaceResearch.com
https://doi.org/10.33263/BRIAC0102.977981
Original Research Article Open Access Journal
Received: 27.12.2019 / Revised: 20.01.2020 / Accepted: 23.01.2020 / Published on-line: 27.01.2020

Formation of boron – silica based mesoporous and studies of its adsorption ability for curcuminoids

Adang Firmansyah [1,2,*], Ilma Nugrahani [1], Komar Ruslan Wirasutisna [1], Slamet Ibrahim [1]
[1] School of Pharmacy, Bandung Institute of Technology, Indonesia
[2] Sekolah Tinggi Farmasi Indonesia, Bandung, Indonesia
*corresponding author e-mail address: ***adangfirmansyah@stfi.ac.id, ilma_nugrahani@yahoo.com*** | Scopus ID 24335737400

ABSTRACT
The development aims of mesoporous silica formation in pharmaceutical fields were its uses as a drug delivery vehicle and in separation. It is possible because of the large particle surface area, the presence of pores, and the possibility to modify functional groups in the mesoporous materials. In this study, the formation of silica-based mesoporous and boron-silica-based mesoporous materials was carried out by sol-gel techniques and modification of functional groups was carried out by the co-condensation method. Mesoporous material characterization was carried out using scanning electron microscopy (SEM), transmission electron microscopy (TEM), and Fourier transform infrared (FTIR). Adsorption ability of curcuminoid onto the mesoporous was carried out through isotherm adsorption study approaches using adsorption models including Langmuir, Freundlich, and Temkin model. The results of the isotherm adsorption study showed that the Freundlich model is the best model for isotherm adsorption with an r^2 value of 0.997.
Keywords: *adsorption isotherm; Langmuir model; Freundlich model; Temkin model; curcuminoid; boron silica mesoporous.*

1. INTRODUCTION

Since its discovery as a catalyst, silica-based mesoporous material was developed both in terms of formation and application. Mesoporous silica formation produced in various forms of material, such as cubic, hexagonal, or other shapes. The formation method also undergoes development as in the case of silica sources such as tetraethylorthosilicate or TEOS, sodium silicate SiO_2, or other alternative sources like rice husk [1].

Various types of surfactants, such as cationic surfactant CTAB, anionic surfactant sodium laurate, triblock copolymer like Pluronic F127, or double surfactant which mix CTAC as a cationic surfactant and Pluronic as an anionic surfactant were used as other sources [2, 3, 4, 5]. Modification of the mesoporous surface for various purposes has been done by introducing amine group through the addition of (3-aminopropyl)triethoxysilane (APTES), Tris(2-aminoethyl)amine (TREN) and tetraethylenepentamine (TEPA), or modification using inorganic compounds like cobalt and molybdenum [2, 6, 7, 8].

Large mesoporous surface area is one reason for its use as an adsorbent, especially for metal compounds as pollutants. Several studies have shown the effectiveness of absorbing metal pollutants like Cu [9, 10].

The nature of inert mesoporous silica (non-toxic) has a large pore volume and surface area, guiding other research studies that have recently begun to develop, namely the use of mesoporous silica as a carrier of medicinal ingredients [11, 12, 13, 14, 15]. Another utilization of silica mesoporous is for the separation of desired molecules by selective adsorption [16].

One of the natural compounds which have been widely used as a medicinal ingredient is curcuminoid which proceeds from the turmeric rhizome. Research studies have shown that curcumin containing in curcuminoids has many pharmacological activities including anti-inflammatory, anti-microbial, wound healing, anti-oxidant, anti-cancer, anti-fungal and also antiviral [17, 18, 19].

The method of separation and isolation of curcumin or curcuminoid has developed using various methods such as thin-layer chromatography (TLC), column chromatography, high-performance liquid chromatography (HPLC), pressurized liquid extraction, and microwave-assisted extraction [20, 21, 22, 23, 24, 25].

However, it is still considered an exhausted, relatively difficult and quite expensive method for preparative purposes. Since mesoporous silica can be used to adsorb natural material compounds, it is possible to use mesoporous silica as a functional material for absorbing curcuminoids. This is considered quite prospective because, in addition to potentially being a separating material, it is also a carrier of the drug [26, 27, 28]. Another study has been done to use mesoporous silica as a drug carrier for curcumin [13]. This research aims to find out how the affinity and effectiveness of absorption as well as the adsorption of curcuminoid on silica and boron-silica mesoporous.

2. MATERIALS AND METHODS

2.1. Instruments.

Thermo Fisher® Nicolet iS5 FTIR spectrometer, Holder of ZnSe iD3 ATR (Attenuated Total Reflectance), JEOL JSM Scanning Electron Microscope (SEM), HITACHI HT7700 Transmission Electron Microscope (TEM), Shimadzu UV-1800 Spectrophotometer.

2.2. Tools.

The tools used in this study were analytical balance, Thermo Scientific® Cimarec hot plate, measuring cylinder, beaker glass, thermometer, stirring rod, and filter paper.

2.3. Materials.

Turmeric samples, curcuminoid standard from the Business Department of Sekolah Tinggi Farmasi Indonesia, cetyltrimethylammonium bromide/CTAB (Amresco), aquadest, ethanol (Merck), ammonia (Merck), tetraethylorthosilicate/TEOS (Merck), boric acid (Merck).

2.4. Research Methods

2.4.1. Silica Mesoporous (MCM) and Boron – Silica Mesoporous Formation

Mesoporous silica (MCM) was prepared using the sol-gel technique. High purity cetyltrimethylammonium bromide (CTAB) as a template, dissolved in mixture of 100 mL of H_2O and 100 mL 96% ethanol under vigorous stirring at 70°C. After adjusting the pH to 10-11 using 25% ammonia, 20 mL tetraethylorthosilicate (TEOS) as a silica source was added dropwise, and the mixture was stirred vigorously for four hours. The mixture was heated for aging at 100°C for 24 hours. The solid product was washed with distilled water until a neutral pH was attained before it was dried at the oven overnight. Removal of organic template was performed by the calcination process at 600°C for eight hours. For boron-silica mesoporous synthesis, 100 mg (BL-MCM), 300 mg (BM-MCM) and 900 mg (BH-MCM) H_3BO_3 were added before the addition of TEOS.

2.4.2. Silica Mesoporous (MCM) and Boron – Silica Mesoporous Characterization

The mesoporous materials formed were characterized by Fourier transform infrared (FTIR), scanning electron microscope (SEM), and transmission electron microscope (TEM). FTIR spectra were taken in Nicolet iS5 Thermo Fisher Spectrometer using the resolution of 4 cm^{-1} in 4000 – 400 cm^{-1} range. Particle morphology was analyzed by SEM using JEOL JSM at a voltage 15 kV. The sample powder was coated with gold to form a conductive layer on a carbon stub to evaluate the surface properties. TEM image was recorded with HITACHI HT7700 at an accelerating voltage of 120 kV to assess the size and shape of the pores of mesoporous silica.

2.4.3. Adsorption Test

Curcuminoid solution was prepared by dissolving curcuminoid in ethanol 96% at the desired concentration. Various concentrations were made using curcuminoid solution and measured by Visible Spectrometer at 403 nm for generating linear regression of the calibration curve for quantitative analysis of curcuminoid. An adsorption test was conducted by mixing 100 mg MCM with 5 mL of various concentrations of curcuminoid 0 ppm to 140 ppm and stirred for 60 minutes. The mixture then stands for 24 hours. Filtrate measured for absorbance at 403 nm using the visible spectrometer.

3. RESULTS

3.1. Mesoporous Characterization

Figure 1 (a) shows FTIR spectra of the unloaded mesoporous silica (MCM) with characteristic vibration bands of Si-O-Si stretch at 1100-1200 cm^{-1}, Si-OH bending at 1600 cm^{-1} and also several silanol bands at 3400-3600 cm^{-1}. Curcumin spectrum in Figure 1 (d) shows functional groups such as hydroxyl, carbonyl, and ethylene at about 3500 cm^{-1}, 1600 cm^{-1}, and 1500 cm^{-1} respectively as the major peaks, and also bending vibration of alkene group at 700-900 cm^{-1}. FTIR spectrum of silica mesoporous curcumin loaded shows in Figure 1 (c) before elution and Figure 1 (b) after elution with acetone. As we can see that spectrum (c) relatively have the same spectrum with curcumin spectrum indicating the effectivity of curcumin adsorption on mesoporous silica, and spectrum (b) is relatively similar to the spectrum (a) which means the curcumin adsorbed can be eluted completely with acetone.

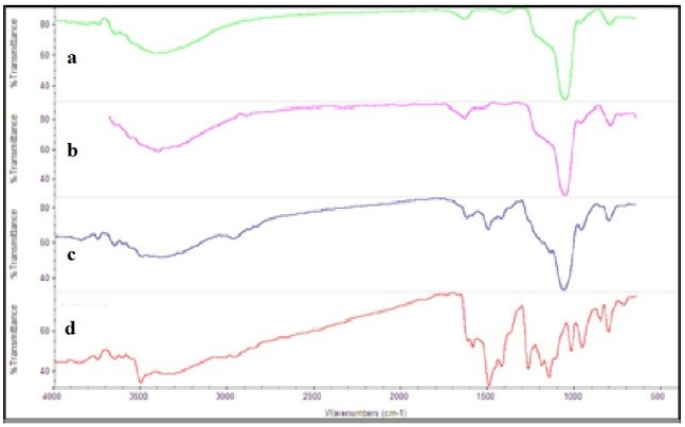

Figure 1. FTIR spectrum of silica mesoporous (a), curcuminoid (d), mesoporous silica with curcuminoid adsorbed (c), and silica mesoporous with curcuminoid adsorbed after elution with acetone (b).

SEM was used for determining the morphology, including shape, size and size distribution of MCM, BL-MCM, BM-MCM and BH-MCM (boron-silica mesoporous with different boron concentration). SEM image shows in Figure 2 indicating that the particle has homogenous shape especially for boron-silica mesoporous compared to silica mesoporous which still show agglomeration. Particle size ranges from 200-600 nm for MCM and 700- 900nm for BL-MCM, BM-MCM, and BH-MCM which means that boron influences the size of the mesoporous material, an increased boron concentration makes the higher sizes of mesoporous.

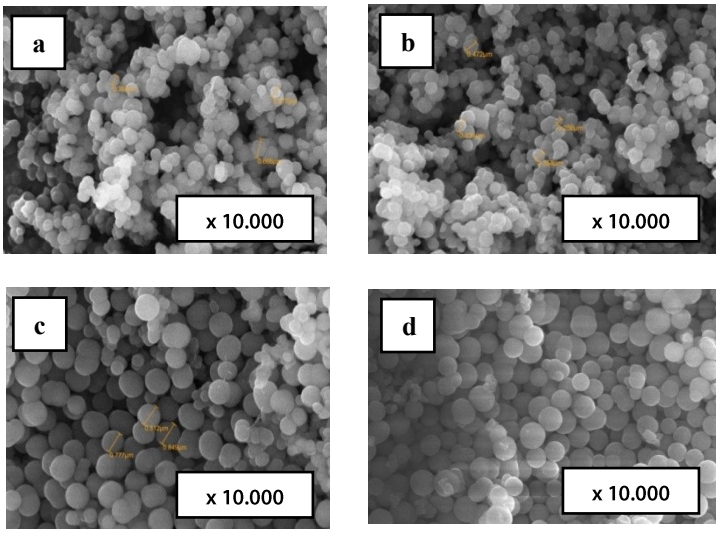

Figure 2. SEM image of silica mesoporous MCM (a), boron-doped silica mesoporous with low concentration BL-MCM (b), middle boron concentration BM-MCM (c), and high boron concentration BH-MCM (d).

Form the TEM image in Figure 3 we can clearly observe a well-ordered hexagonal shaped pore structure in particular for

MCM and BL-MCM, while for higher boron concentration in BM-MCM and BH-MCM have more irregular shape although the hexagonal shape of pore structure still can be observed. The pore size ranges between 5-20 nm for MCM and BL-MCM, but for BM-MCM and BH-MCM we can find that pore size range between 1-5 nm, which means higher boron concentrations tend to make smaller pore sizes.

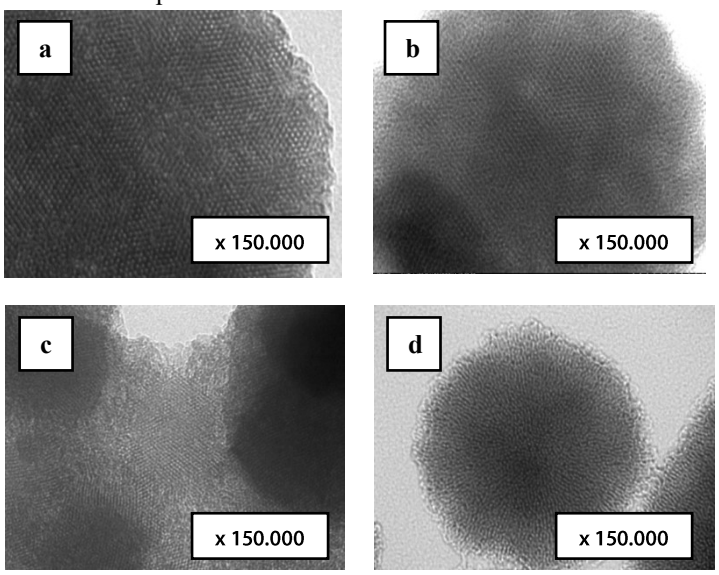

Figure 3. TEM image of silica mesoporous MCM (a), boron-doped silica mesoporous with low concentration BL-MCM (b), middle boron concentration BM-MCM (c), and high boron concentration BH-MCM (d).

3.2. Adsorption Isotherms

3.2.1. Langmuir adsorption isotherm.

Langmuir model is an empirical model for monolayer adsorption, which can be formulated as the equation:

$$q_e = \frac{Q_o K_L C_e}{1 + K_L C_e} \quad (1)$$

Linear form: $\frac{1}{q_e} = \frac{1}{Q_o} + \frac{1}{Q_o K_L C_e}$ (2)

Ce : the equilibrium concentration of adsorbate (mg/L^{-1})
qe : amount of curcuminoid adsorbed at equilibrium (mg/g)
Qo : maximum monolayer coverage capacity (mg/g)
K_L : Langmuir constant (L/mg)

q_{max} and K_L were generated from the slope and intercept of Langmuir plot $\frac{1}{q_e}$ vs $\frac{1}{C_e}$.

The Langmuir model describes the formation of a monolayer adsorbate on the outer surface of the adsorbent quantitatively, after that no further adsorption takes place. Langmuir represents the equilibrium adsorbate distribution between the solid and liquid phases and is considered valid for monolayer adsorption onto a surface containing a finite number of identical sites and assumes uniform energy of adsorption onto the surface. The fitting was carried out by plotting 1/*qe* versus 1/*Ce.* The value of *qmax* and K_L were determined from the slope and intercept of that Langmuir plot. The essential features of the Langmuir isotherm may be expressed in terms of equilibrium parameter R_L, which is a dimensionless constant referred to as the separation factor [29].

$$R_L = \frac{1}{1+(K_L C_o)} \quad (3)$$

where:

Co : initial concentration
K_L : Langmuir constant

R_L value indicates the adsorption nature to be either unfavorable if $R_L > 1$, linear if $R_L = 1$, favorable if $0 < R_L < 1$, and irreversible if $R_L = 0$. From the results in Table 1, R_L (the separation factor) of all mesoporous materias is greater than zero but less than one, indicating that the Langmuir isotherm is favorable. R_L value are 0.924 (MCM), 0.672 (BL-MCM), 0.790 (BM-MCM), and 0.739 (BH-MCM). R_L value of MCM is the closest to one, indicating that the equilibrium adsorption of MCM was the most favorable. The maximum monolayer coverage capacity (q_m) from the Langmuir isotherm model was determined to be 3.1619 mg/g (MCM), 8.558 mg/g (BL-MCM), 4.3223 mg/g (BM-MCM), and 8.8973 mg/g (BH-MCM). K_L (Langmuir isotherm constant) are 0.026 L/mg (MCM), 0.057 L/mg (BL-MCM), 0.0616 L/mg (BM-MCM), and 0.0397 L/mg (BH-MCM). The r^2 value of MCM is the closest to one, indicating that the adsorption data of MCM is the best to be fitted to the Langmuir isotherm model.

3.2.2. Freundlich adsorption isotherm.

Freundlich model is an empirical model for multilayer adsorption, which can be formulated as the equation:

$$q_e = K_F C_e^{\frac{1}{n}} \quad (4)$$

Linear form: $log\ q_e = log\ K_F + \frac{1}{n} log C_e$ (5)

K_F : Freundlich constant
n : adsorption intensity

This model is applicable to describe the adsorption characteristics of the heterogeneous surface. The constant *Kf* in the Freundlich equation is an approximate indicator of adsorption capacity. The *1/n* value is a function of adsorption intensity, indicating the strength of adsorption in the adsorption process. If *n* = 1, then the partition between the two phases are independent of the concentration. If the value of 1/*n* is below one, it indicates normal adsorption. On the other hand, if the value of 1/*n* is above one, it indicates cooperative adsorption. The lower the value of 1/*n*, the higher the expected heterogeneity of the adsorbent surface. This expression can be reduced to a linear adsorption isotherm when 1/*n* = 1. If *n* lies between one and ten, this indicates a favorable sorption process [29].

From the results in Table 1, the value of 1/*n* are 0.8652 (MCM), 0.9317 (BL-MCM), 0.8109 (BM-MCM), and 0.9673 (BH-MCM), while *n* are 1.1558 (MCM), 1.0733 (BL-MCM), 1.2332 (BM-MCM), and 1.0338 (BH-MCM). The *n* value lies between one and ten, indicating that the adsorption of curcuminoid onto all mesoporous materials are favorable. The higher the *n* value, the stronger the adsorption intensity. The *n* value of BM-MCM is the highest of all mesoporous materials, indicating that the adsorption process with BM-MCM has the strongest adsorption intensity. The r^2 value of MCM is the closest to one, indicating that the adsorption data of MCM is the best to be fitted to the Freundlich isotherm model.

3.2.3. Temkin adsorption isotherm.

Temkin model is an empirical model for adsorption with pore-filling mechanism, which can be illustrated as the equation :

$$q_e = \frac{RT}{b} ln\ (A_\tau C_e) \quad (6)$$

$$q_e = \frac{RT}{b} ln\ A_\tau + \left(\frac{RT}{b}\right) ln\ C_e \quad (7)$$

$$\frac{RT}{b} = B$$

Linear form : $q_e = B\ ln\ A_\tau + B\ ln\ C_e$ (8)

Aτ : Temkin equilibrium binding constant (L/g)
B : Temkin constant
R : gas constant
T : temperature at 298 K
B : constant related to the heat of sorption (J/mol)

This model contains a factor that takes into account adsorbent-adsorbate interactions on the adsorption process. By ignoring the extremely low and large value of concentrations, the model assumes that the heat of adsorption (ΔH_{ads}, a function of temperature) of all molecules in the layer decreases linearly rather than in a logarithmic manner with the coverage. The adsorption is characterized by a uniform distribution of binding energies, up to maximum binding energy. The fitting was carried out by plotting the quantity sorbed *qe* versus ln *Ce*. The constants were determined from the slope and the intercept of that Temkin plot [29].

From the results in Table 1, the A_τ values were 0.1169 L/g (MCM), 0.0942 L/g (BL-MCM), 0.1120 L/g (BM-MCM), and 0.0893 L/g (BH-MCM). The highest A_τ value of MCM corresponding to the highest maximum binding energy of all mesoporous materials. The *B* values were 7.7447 J/mol (MCM), 3.8016 J/mol (BL-MCM), 4.8394 J/mol (BM-MCM), and 4.1867 J/mol (BH-MCM). The *b* values, related to the variation of adsorption energy in the Temkin model, were 319.92 J/mol (MCM), 651.76 J/mol (BL-MCM), 511.99 J/mol (BM-MCM), and 591.81 J/mol (BH-MCM). The constant *b* for all mesoporous materials were positive. This value indicates that the adsorption reaction is exothermic. The r^2 values are 0.8895 (MCM), 0.8445 (BL-MCM), 0.8617 (BM-MCM), and 0.8267 (BH-MCM). Based on these r^2 values, the Temkin model showed a worse fit for adsorption data than Langmuir and Freundlich models.

Table 1. Langmuir, Freundlich, and Temkin isotherm parameters of linear fitting for four adsorbents.

Model	Parameter	MCM	BL-MCM	BM-MCM	BH-MCM
Langmuir	q_m	3.1619	8.558	4.3223	8.8973
	r^2	0.9866	0.9513	0.9377	0.9692
	K_L	0.026	0.057	0.0616	0.0397
	R_L	0.924	0.672	0.790	0.739
Freundlich	K_F	0.3784	0.1174	0.2833	0.1070
	n	1.1558	1.0733	1.2332	1.0338
	r^2	0.997	0.9681	0.981	0.9831
Temkin	A_τ	0.1169	0.0942	0.1120	0.0893
	b	319.9236	651.7552	511.9876	591.8056
	r^2	0.8895	0.8445	0.8617	0.8267
	B	7.7447	3.8016	4.8394	4.1867

4. CONCLUSIONS

Synthesized mesoporous silica and mesoporous boron-silica showed a homogeneous round particle with a size of 200 – 900 nm,with increasing boron concentrations resulting in larger particle size. Mesoporous particles showed the formation of hexagonal pores with a size of 1 – 20 nm. Increasing boron concentration results in a smaller pore size.

Adsorption effectiveness of curcuminoids onto the mesoporous using three models (Langmuir, Freundlich, and Temkin) showed that only Langmuir and Freundlich models are in accordance with the adsorption data, which r^2 values for Langmuir, Freundlich, and Temkin respectively were 0.9866, 0.997, 0.8895 for MCM; 0.9513, 0.9681, 0.8445 for BL-MCM; 0.9377, 0.981, 0.8617 for BM-MCM; and 0.9692, 0.9831, 0.8267 for BH-MCM. Based on the results, it can be concluded that the Freundlich model of MCM is the best model for isotherm adsorption with an r^2 value of 0.997.

5. REFERENCES

1. Purnawira, B.; Purwaningsih, H.; Ervianto, Y.; Pratiwi, V.M.; Susanti, D.; Rochiem, R.; Purniawan, A. Synthesis and characterization of mesoporous silica nanoparticles (MSNp) MCM 41 from natural waste rice husk, IOP Conference Series: Materials Science and Engineering, Tangerang Selatan, Indonesia, 25-26 September 2018; IOP Publishing: Bristol, United Kingdom, 2019.
2. Xueao, Z.; Wu, W.; Wang, J.; Tian, X. Direct synthesis and characterization of highly ordered functional mesoporous silica thin films with high amino-groups content. *Applied Surface Science* **2008**, 254, 2893-2899, https://doi.org/10.1016/j.apsusc.2007.10.022.
3. Kong, L.; Liu, S.; Yan, X.; Li, Q.; He, H. Synthesis of hollow-shell MCM-48 using the ternary surfactant templating method. *Microporous and Mesoporous Materials* **2005**, 81, 251-257, https://doi.org/10.1016/j.micromeso.2005.02.011.
4. Bitrus, A. B.; Wyasu, G. Sol-gel preparation and synthesis of mesoporous silica using de-ionised water as solvent and poly(ethylene-glycol)-block-poly(propylene-glycol)-block-poly(ethylene-glycol) as source of micelle. *International Journal of Scientific and Engineering Research* **2014**, 5, 1112-1115.
5. Suzuki, K.; Ikari, K.; Imai, H. Synthesis of Silica Nanoparticles Having a Well-Ordered Mesostructure Using a Double Surfactant System. *Journal of the American Chemical Society* **2004**, 126, 462-463, https://doi.org/10.1021/ja038250d.
6. Bhagiyalakshmi, M.; Yun, L.J.; Anuradha, R.; Jang, H.T. Utilization of rice husk ash as silica source for the synthesis of mesoporous silicas and their application to CO_2 adsorption through TREN/ TEPA grafting. *Journal of Hazardous Materials* **2010**, 175, 928-938, https://doi.org/10.1016/j.jhazmat.2009.10.097.
7. Masykuroh, A.; Trisunaryanti, W.; Falah, I.I.; Sutarno. Preparation and Characterization of Co and Co-Mo Loaded on Mesoporous Silica for Hydrocracking of Waste Lubricant. *International Journal of ChemTech Research* **2016**, 9, 598-606.
8. Li, Y.; Song, F.; Guo, Y.; Cheng, L.; Chen, Q. Multifunctional Amine Mesoporous Silica Spheres Modified with Multiple Amine as Carriers for Drug Release. *Journal of Nanomaterials* **2018**, 2018, 1-10, https://doi.org/10.1155/2018/1726438.
9. Mureseanu, M.; Cioatera, N.; Trandafir, I.; Georgescu, I.; Fajula, F.; Galarneau, A. Selective Cu^{2+} adsorption and recovery from contaminated water using mesoporous hybrid silica bio-adsorbents. *Microporous and Mesoporous Materials* **2011**, 146, 141-150, https://doi.org/10.1016/j.micromeso.2011.04.026.

10. Alothman, Z.A.; Apblett, A.W. Preparation of mesoporous silica with grafted chelating agents for uptake of metal ions. *Chemical Engineering Journal* **2009**, 155, 916-924, https://doi.org/10.1016/j.cej.2009.09.028
11. Slowing, I.I.; Vivero-Escoto, J.L.; Wu, C.W.; Lin, V.S.Y. Mesoporous silica nanoparticles as controlled release drug delivery and gene transfection carriers. *Advanced Drug Delivery Reviews* **2008**, 60, 1278-1288, https://doi.org/10.1016/j.addr.2008.03.012
12. Manzano, M.; Aina, V.; Areán, C.O.; Balas, F.; Cauda, V.; Colilla, M.; Delgado, M.R.; Vallet-Regí, M. Studies on MCM-41 mesoporous silica for drug delivery: Effect of particle morphology and amine functionalization. *Chemical Engineering Journal* **2008**, 137, 30-37, https://doi.org/10.1016/j.cej.2007.07.078.
13. Bolouki, A.; Rashidi, L.; Vasheghani-Farahani, E.; Piravi-Vanak, Z. Study of Mesoporous Silica Nanoparticles as Nanocarriers for Sustained Release of Curcumin. *Int. J. Nanosci. Nanotechnol*. **2015**, 11, 139-146.
14. Liu, Y.; Miyoshi, H.; Nakamura, M. Novel drug delivery system of hollow mesoporous silica nanocapsules with thin shells: Preparation and fluorescein isothiocyanate (FITC) release kinetics. *Colloids and Surfaces B: Biointerfaces* **2007**, 58, 180-187, https://doi.org/10.1016/j.colsurfb.2007.03.005
15. Yang, K.N.; Zhang, C.Q.; Wang, W.; Wang, P.C.; Zhou, J.P.; Liang, X. J. pH-responsive mesoporous silica nanoparticles employed in controlled drug delivery systems for cancer treatment. *Cancer Biology Medicine* **2014**, 11, 34-43, https://doi.org/10.7497/j.issn.2095-3941.2014.01.003.
16. Alothman, Z.A. A Review: Fundamental Aspects of Silicate Mesoporous Materials. *Materials* **2012**, 5, 2874-2902, https://doi.org/10.3390/ma5122874.
17. Maheshwari, R.K.; Singh, A.K.; Gaddipati, J.; Srimal, R.C. Multiple biological activities of curcumin: A short review. *Life Sciences* **2006**, 78, 2081-2087, https://doi.org/10.1016/j.lfs.2005.12.007.
18. Hatcher, H.; Planalp, R.; Cho, J.; Torti, F.M.; Torti, S.V. Curcumin: From ancient medicine to current clinical trials. *Cell. Mol. Life Sci.* **2008**, 65, 1631-1652, https://doi.org/10.1007/s00018-008-7452-4.
19. Moghadamtousi, S.Z.; Kadir, H.A.; Hassandarvish, P.; Tajik, H.; Abubakar, S.; Zandi, K. A Review on Antibacterial, Antiviral, and Antifungal Activity of Curcumin. *BioMed Research International* **2014**, 2014, 1-12, http://dx.doi.org/10.1155/2014/186864
20. Péret-Almeida, L.; Cherubino, A.P.F.; Alves, R.J.; Dufossé, L.; Glória, M.B.A. Separation and determination of physico-chemical characteristics of curcumin, demethoxycurcumin and bisdemethoxycurcumin. *Food Research International* **2005**, 38, 1039-1044, https://doi.org/10.1016/j.foodres.2005.02.021.
21. Pawar, H.A.; Gavasane, A.J.; Choudhary, P.D. A Novel and Simple Approach for Extraction and Isolation of Curcuminoids from Turmeric Rhizomes. *Natural Products Chemistry and Research* **2018**, 6, 1-4, https://doi.org/10.4172/2329-6836.1000300.
22. Wulandari, R.; Sudjadi; Martono, S.; Rohman, A. Liquid Chromatography and Fourier Transform Infrared Spectroscopy for quantitative analysis of individual and total curcuminoid in *Curcuma longa* extract. *Journal of Applied Pharmaceutical Science* **2018**, 8, 107-113, https://doi.org/10.7324/JAPS.2018.8916.
23. Cahyono, B.; Ariani, J.; Failasufa, H.; Suzery, M.; Susanti, S.; Hadiyanto, H. Extraction of Homologous Compounds of Curcuminoid Isolated from Temulawak (*Curcuma xanthorriza Roxb.*) Plant. *Rasayan Journal of Chemistry* **2019**, 12, 7-13, http://dx.doi.org/10.31788/RJC.2019.1213092.
24. Chao, I.C.; Wang, C.M.; Li, S.P.; Lin, L.G.; Ye, W.C.; Zhang, Q.W. Simultaneous Quantification of Three Curcuminoids and Three Volatile Components of *Curcuma longa* Using Pressurized Liquid Extraction and High-Performance Liquid Chromatography. *Molecules* **2018**, 23, 1-9, https://doi.org/10.3390/molecules23071568.
25. Lateh, L.; Yuenyongsawad, S.; Chen, H.; Panichayupakaranant, P. A green method for preparation of curcuminoid-rich *Curcuma longa* extract and evaluation of its anticancer activity. *Pharmacognosy Magazine* **2019**, 15, 730-735, https://doi.org/10.4103/pm.pm_162_19.
26. Li, T.; Shi, S.; Goel, S.; Shen, X.; Xie, X.; Chen, Z.; Zhang, H.; Li, S.; Qin, X.; Yang, H.; Wu, C.; Liu, Y. Recent advancements in mesoporous silica nanoparticles towards therapeutic applications for cancer. *Acta Biomaterialia* **2019**, 89, 1-13, https://doi.org/10.1016/j.actbio.2019.02.031.
27. Manzano, M.; Vallet-Regí, M. Mesoporous Silica Nanoparticles for Drug Delivery. *Advanced Functional Materials* **2019**, 2019, 1-13, https://doi.org/10.1002/adfm.201902634.
28. Narayan, R.; Nayak, U.Y.; Raichur, A.M.; Garg, S. Mesoporous Silica Nanoparticles: A Comprehensive Review on Synthesis and Recent Advances. *Pharmaceutics* **2018**, 10, 1-49, https://doi.org/10.3390/pharmaceutics10030118.
29. Dada A.O.; Olalekan, A.P.; Olatunya, A.M.; Dada, O. Langmuir, Freundlich, Temkin and Dubinin–Radushkevich Isotherms Studies of Equilibrium Sorption of Zn^{2+} Unto Phosphoric Acid Modified Rice Husk. *IOSR Journal of Applied Chemistry* **2012**, 3, 38-45, https://doi.org/10.9790/5736-0313845.

6. ACKNOWLEDGEMENTS

The author would like to thank Hazanah Foundation for the research funding, to Bandung Institute of Technology for facilitating the use of Scanning Electron Microscope (SEM) and Transmission Electron Microscope (TEM), and to Sekolah Tinggi Farmasi Indonesia for facilitating the use of Fourier Transform Infrared (FTIR) spectroscopy.